Theoretical Computer Science 893 (2021) 1–16

Contents lists available at ScienceDirect

Theoretical Computer Science

www.elsevier.com/locate/tcs

Long lived transients in gene regulation

Tatjana Petrov [a,b,*], Claudia Igler [d,c], Ali Sezgin [c], Thomas A. Henzinger [c], Calin C. Guet [c]

[a] Department of Computer and Information Science, University of Konstanz, 78464 Konstanz, Germany
[b] Centre for the Advanced Study of Collective Behaviour, University of Konstanz, 78464 Konstanz, Germany
[c] IST Austria, Am Campus 1, 34000 Klosterneuburg, Austria
[d] Institute of Integrative Biology, Universitätsstrasse 16, ETH Zurich, 8092 Zurich, Switzerland

ARTICLE INFO

Article history:
Received 7 August 2020
Received in revised form 15 March 2021
Accepted 19 May 2021
Available online 4 June 2021

Keywords:
Gene regulation
Stochastic modelling
Transient memory
Long lived transients
Finite state dynamical systems
DNA looping
Rule-based modelling

ABSTRACT

Gene expression is regulated by the set of transcription factors (TFs) that bind to the promoter. The ensuing regulating function is often represented as a combinational logic circuit, where output (gene expression) is determined by current input values (promoter bound TFs) only. However, the simultaneous arrival of TFs is a strong assumption, since transcription and translation of genes introduce intrinsic time delays and there is no global synchronisation among the arrival times of different molecular species at their targets. We present an experimentally implementable genetic circuit with two inputs and one output, which in the presence of small delays in input arrival, exhibits qualitatively distinct population-level phenotypes, over timescales that are longer than typical cell doubling times. From a dynamical systems point of view, these phenotypes represent long-lived transients: although they converge to the same value eventually, they do so after a very long time span. The key feature of this toy model genetic circuit is that, despite having only two inputs and one output, it is regulated by twenty-three distinct DNA-TF configurations, two of which are more stable than others (DNA looped states), one promoting and another blocking the expression of the output gene. Small delays in input arrival time result in a majority of cells in the population quickly reaching the stable state associated with the first input, while exiting of this stable state occurs at a slow timescale. In order to mechanistically model the behaviour of this genetic circuit, we used a rule-based modelling language, and implemented a grid-search to find parameter combinations giving rise to long-lived transients. Our analysis shows that in the absence of feedback, there exist path-dependent gene regulatory mechanisms based on the long timescale of transients. The behaviour of this toy model circuit suggests that gene regulatory networks can exploit event timing to create phenotypes, and it opens the possibility that they could use event timing to memorise events, without regulatory feedback. The model reveals the importance of (i) mechanistically modelling the transitions between the different DNA-TF states, and (ii) employing transient analysis thereof.

* Corresponding author at: Department of Computer and Information Science, University of Konstanz, 78464 Konstanz, Germany.
E-mail addresses: tatjana.petrov@gmail.com (T. Petrov), claudia.igler@env.ethz.ch (C. Igler), ali.sezgin.cs@gmail.com (A. Sezgin), tah@ist.ac.at (T.A. Henzinger), calin@ist.ac.at (C.C. Guet).

https://doi.org/10.1016/j.tcs.2021.05.023

1. Introduction

The fundamental conceptual breakthroughs related to how a gene is turned on and off, have inspired a large body of theoretical and experimental work on gene regulation, including the explanation of stochastic switching between lysis and lysogeny of phage [1], all the way to more complex logic gate formalisms that attempt to abstract more complex biological behaviour. Synthetic biology enthusiasts often use analogies with how electronic circuits are manipulated by computers [2,3], and have demonstrated success in engineering simple genetic circuits that are encoded in DNA and perform their function *in vivo*. However, such digital (in the sense that the expression states are encoded through Boolean values) and combinational design (in the sense that the output is a pure function of present input only, different to the *sequential* design) quickly becomes infeasible in experiment, because the cellular environment is resource-limited and highly crosstalk-prone [4]. The effective engineering of biological systems needs to take into account the intrinsic properties of the biological medium, so as not to fight against the principles of tinkering that characterise biology [5], but rather to make use of them [6]. Significant conceptual challenges remain related to the still unsatisfactory quantitative but also qualitative understanding of the underlying processes [7,2]. Understanding time-dependent phenomena is fundamental in this complex picture of the cell that unravels itself at the molecular scale, especially since cells do not have computer-like clocking mechanisms, beyond circadian and cell cycle ones. A major question emerges as to what are the macroscopic effects of small delays in the arrival times of different molecules at molecular targets.

Gene expression in a single cell is regulated by stochastic switching among possible configurations at the DNA (the architectural configuration of which is often termed *promoter logic*), and their effect on the copy number of other species involved in regulation, such as mRNA, proteins and transcription factors (TFs). Consequently, the number of possible molecular configurations in the promoter logic (of the DNA) grows combinatorially with the number of operator sites regulating the gene in question. For instance, the mechanism that underlies the genetic switch of bacteriophage lambda, that contains three left and three right operators for the CI protein in the left and right promoters (PL and PR), leads to 1200 different DNA-TF configurations [8]. The combinatorial explosion of the number of possible configurations makes the model tedious to even write down, let alone execute and make predictions about it. The switching mechanism depends on the binding affinities of the TFs and RNA polymerase to their respective binding sites as well as the concentrations of those proteins in the cell [9]. The induced stochastic process enumerates states which couple the configuration of the DNA, with the copy number of the protein, and possibly other species involved in regulation, such as mRNA and TFs. In order to faithfully predict the stochastic evolution of the gene product (protein) over time, the modelled system can be solved numerically, by integrating the Master equation of the stochastic process. change this sentence This is often prohibitive in practice, due to large dimensionality and a combinatorial number of reachable states. For this reason, modelling practice often abstracts away details and adds assumptions. A lightweight approach is simulating the system by Gillespie simulation [10] and statistically inferring the protein expression profile, hence trading off accuracy and precision. Other approaches are based on mean-field approximations (e.g. deterministic limit [11] and linear-noise approximation [12]), significantly reducing the computational effort. However, mean-field models do not capture the inherent stochasticity, which is especially prominent in gene regulation. Further model reduction ideas exploit multi-scaleness of the system: fast subsystems are identified (possibly dynamically), and assumed to be reaching an equilibrium fast, relative to the observable dynamics [13–16]. A special class of reductions based on steady-state assumption is the widely used approach of *statistical thermodynamics limit*. This widely and successfully used method (e.g. [17–19]) estimates the probability of being in any of the possible DNA binding configurations from their relative binding energies (Boltzmann weights) and the protein concentrations, both of which can often be experimentally accessed. The statistical thermodynamics limit model is rooted in the argument that, when the switching rates among DNA configurations are fast, the probability distribution over the configurations is rapidly arriving at its stationary distribution. While this model takes into account the stochasticity inherent to the DNA-TF binding configurations, it neglects their transient evolution, before the equilibrium is reached. It abstracts away the relative speed of rates of different reactions at the DNA, and how they connect to one another. The question arises: In which ways does the transient regime at the DNA (promoter) affect the shape and duration of observable protein dynamics? Can it happen that the observable transients move towards the unique equilibrium so slowly, that they are mistaken for steady-state dynamics?

In this paper, we first present our proof-of-concept genetic circuit based on two different transcription factors which regulate the same gene, without feedback. This circuit, first introduced in [20], suggests that the genetic circuit can memorise the order of arrival of TFs, although there is no explicit feedback at the gene regulatory level. It is realistic, experimentally implementable in the sense that the mechanism can be implemented by the current technology and kinetic rate values are in realistic ranges. Such transient, dynamic memory is effectuated through *long lived transients*, transient phenotypes which appear to be stable even though they are not, for extraordinarily long times [21]. We extend [20] with insights towards a general characterisation of promoter networks which exhibit long lived transients. Concretely, we discuss a generic scenario where a single protein is regulated through a network of DNA-TF binding states, without feedback, and describe which of them more efficiently extend the average return time in promoter states. One of the DNA-TF binding states with long lived transients was recently used to demonstrate the phenomenon - 'slow-by-fast' transients (where, counter-intuitively, accelerating all reactions at the promoter, slows down the transient and increases noise of the protein) [22].

The paper is organised as follows. In Section 2, we introduce the mechanistic modelling of gene regulatory circuits equipped with semantics of stochastic chemical kinetics. In Subsection 2.1, we prove properties relevant for the special case of modelling gene expression without feedback. In Section 3, we introduce the prototype circuit, quantification of long lived

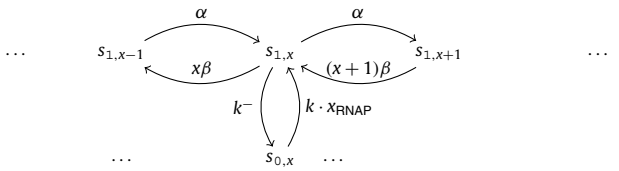

Fig. 1. Transitions of the CTMC underlying basal gene expression. The state space $S \cong \{0,1\} \times \{0,1,2,\ldots\}$, such that $s_{1,x}$ denotes an active configuration (where the RNAP is bound to the DNA) and $x \in \mathbf{N}$ protein molecules.

transients, and the details of parameter search. In Section 4, we summarise the resulting observations from the prototype circuit. Finally, in Section 5, we discuss long lived transients in a general setup of an arbitrary promoter architecture, and we discuss the contributions in 6.

2. Preliminaries and background

A gene is expressed at a basal rate, whenever the RNA polymerase (RNAP) is bound to its promoter region at the DNA. *Activators* are transcription factors (TFs) that bind to specific locations on the DNA, or to other TFs, and enhance the expression of gene g by promoting the binding of RNAP. *Repressors* reduce the expression of gene g, by directly blocking the binding of RNAP, or indirectly, by inhibiting the activators, or promoting direct repressors. The mechanism of how and at which rates the molecular species are interacting is transparently written in a list of reactions. Reactions are equipped with the stochastic semantics which is valid under mild assumptions [23].

Definition 1. A reaction system is a pair (S, R), such that $\mathsf{S} = \{S_1, \ldots, S_n\}$ is a finite set of species, and $\mathsf{R} = \{\mathsf{r}_1, \ldots, \mathsf{r}_r\}$ is a finite set of reactions. The state of a system can be represented as a multi-set of species, denoted by $\mathbf{x} = (x_1, ..., x_n) \in \mathbf{N}^n$. Each reaction is a triple $\mathsf{r}_j \equiv (\mathbf{a}_j, \boldsymbol{\nu}_j, c_j) \in \mathbf{N}^n \times \mathbf{N}^n \times \mathbb{R}_{\geq 0}$, written down in the following form:

$$a_{1j}S_1, \ldots, a_{nj}S_n \xrightarrow{c_j} a'_{1j}S_1, \ldots, a'_{nj}S_n, \text{ such that } \forall i.a'_{ij} = a_{ij} + \nu_{ij},$$

where the vectors $\mathbf{a}_j$ and $\mathbf{a}'_j$ are respectively the *consumption* and *production* vectors due to jth reaction, vector $\boldsymbol{\nu}_j$ specifies the net-change upon the reaction r_j (if the jth reaction occurs, after being in state $\mathbf{x}$, the next state will be $\mathbf{x}' = \mathbf{x} + \boldsymbol{\nu}_j$, and it can occur only if sufficiently many reactants are available, i.e. $x_i \geq a_{ij}$ for $i = 1, \ldots, n$). Finally, c_j is the respective *kinetic rate*.

Stochastic semantics. The species multiplicities follow a continuous-time Markov chain (CTMC) $\{X(t)\}_{t \geq 0}$, defined over the state space $S = \{\mathbf{x} \mid \mathbf{x}$ is reachable from $\mathbf{x}_0$ by a finite sequence of reactions from $\{\mathsf{r}_1, \ldots, \mathsf{r}_r\}\}$. In other words, the probability of moving to the state $\mathbf{x} + \boldsymbol{\nu}_j$ from $\mathbf{x}$ after time Δ is

$$\mathsf{P}(X(t+\Delta) = \mathbf{x} + \nu_j \mid X(t) = \mathbf{x}) = \lambda_j(\mathbf{x})\Delta + o(\Delta),$$

with λ_j the propensity of jth reaction, assumed to follow the principle of mass-action: $\lambda_j(\mathbf{x}) = c_j \prod_{i=1}^{n} \binom{x_i}{a_{ij}}$, and $\frac{o(\Delta)}{\Delta}$ negligible for infinitesimally small Δ. The binomial coefficient $\binom{x_i}{a_{ij}}$ reflects the probability of choosing a_{ij} molecules of species S_i out of x_i available ones.

Example 1 *(Basal gene expression).* Basal gene expression with RNAP binding can be modelled with four reactions, where the first reversible reaction models binding between the promoter site at the DNA and the polymerase, and the second two reactions model the protein production and degradation, respectively:

$$\mathsf{DNA}, \mathsf{RNAP} \leftrightarrow \mathsf{DNA.RNAP} \text{ at rates } k, k^-$$
$$\mathsf{DNA.RNAP} \rightarrow \mathsf{DNA.RNAP} + \mathsf{P} \text{ at rate } \alpha$$
$$\mathsf{P} \rightarrow \emptyset \text{ at rate } \beta.$$

The state space of the underlying CTMC $S \cong \{0,1\} \times \{0,1,2,\ldots\}$, such that $s_{(1,x)} \in S$ denotes an active configuration (where the RNAP is bound to the DNA) with $x \in \mathbf{N}$ protein copy number, as depicted in Fig. 1.

Example 2 *(Adding repression).* Repressor blocking the polymerase binding can be modelled by adding a reaction

$$\mathsf{DNA}, R \leftrightarrow \mathsf{DNA}.R$$

In this case, there are three possible promoter configurations, that is, $S \cong \{\mathsf{DNA}, \mathsf{DNA.RNAP}, \mathsf{DNA}.R\} \times \{0,1,2,\ldots\}$, where $D_0 = \{\mathsf{DNA}, \mathsf{DNA}.R\}$ are inactive promoter states.

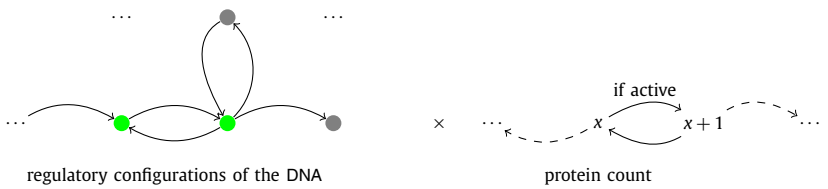

Fig. 2. Each binding configuration of the DNA can be active (green, polymerase bound) or inactive (gray, polymerase not bound). Protein count can increase only when the DNA configuration is active. (For interpretation of the colours in the figure(s), the reader is referred to the web version of this article.)

Computing the transient. Using the vector notation $\mathbf{X}(t) \in \mathbf{N}^n$ for the marginal of process $\{X(t)\}_{t\geq 0}$ at time t, we can compute this transient distribution by integrating the *chemical master equation* (CME). Denoting by $p^{(t)}(\mathbf{x}) = \mathsf{P}(\mathbf{X}(t) = \mathbf{x})$, the CME for state $\mathbf{x} \in \mathbf{N}^n$ reads

$$\frac{\mathrm{d}}{\mathrm{d}t} p^{(t)}(\mathbf{x}) = \sum_{j=1, \mathbf{x}-\boldsymbol{\nu}_j \in \mathsf{S}}^{r} \lambda_j(\mathbf{x} - \boldsymbol{\nu}_j) p^{(t)}(\mathbf{x} - \boldsymbol{\nu}_j) - \sum_{j=1}^{r} \lambda_j(\mathbf{x}) p^{(t)}(\mathbf{x}). \tag{1}$$

The solution may be obtained by solving the system of differential equations, but, due to its high (possibly infinite) dimensionality, it is often statistically estimated by simulating the traces of $\{X_t\}$, known as the stochastic simulation algorithm (SSA) in chemical literature [23]. As the statistical estimation often remains computationally expensive for desired accuracy, for the case when the deterministic model is unsatisfactory due to the low multiplicities of many molecular species [24], different further approximation methods have been proposed, major challenge to which remains the quantification of approximation accuracy (see [25] and references therein for a thorough review on the subject).

2.1. Transients in gene expression without feedback

We will further focus on regulation of single gene without feedback. In the context of a circuit, where TFs are inputs and the population is the average. Since there is a single DNA molecule per cell, each state counts one copy of the current DNA configuration, and zero copies of all other DNA binding configurations. Hence, the expression state for a single gene of interest consists of two layers: the proteins that we see, and the regulatory configuration of the DNA (for example, two activators and polymerase are bound) (Fig. 2). Such two-layer model allows us to study the transient of coupled promoter state and protein count. In order to focus our analysis on the effect of input timing perturbations, yet to keep our model simple, we chose not to involve further mechanistic details, such as the steps involving mRNA.

The following observation states that in general, when there is no feedback, computing the output does not require integrating the Master equation for the entire CTMC, but only for a CTMC controlling the switching among the DNA configurations (depicted left in Fig. 2).

Lemma 1. *Let $\{X(t)\}_{t\geq 0}$ be the CTMC for a model of single gene regulation without feedback, over the state space $S = S_0 \uplus S_1 = (D_0 \uplus D_1) \times \{0, 1, \ldots\}$, where $D_0 = \{\mathsf{D}_{01}, \mathsf{D}_{02}, \ldots\}$ are inactive* DNA *configurations, and $D_1 = \{\mathsf{D}_{11}, \mathsf{D}_{12}, \ldots\}$ are active* DNA *configurations (*RNAP *bound). Let the reaction system* (S, R) *be such that all reactions are of one of the following types (for some $i \geq 0$ and $j \geq 0$):*

$$\begin{aligned}
\textit{(de)activation:}\ & \mathsf{D}_{0i} \leftrightarrow \mathsf{D}_{1i} \textit{ at rates } k_i, k_i^- \\
\textit{switching:}\ & \mathsf{D}_{0i} \leftrightarrow \mathsf{D}_{0j} \textit{ at rates } k_{0ij}, k_{0ij}^- \\
\textit{switching:}\ & \mathsf{D}_{1i} \leftrightarrow \mathsf{D}_{1j} \textit{ at rates } k_{1ij}, k_{1ij}^- \\
\textit{protein synthesis:}\ & \mathsf{D}_{1i} \to \mathsf{D}_{1i} + \mathsf{P} \textit{ at rate } \alpha \\
\textit{protein degradation:}\ & \mathsf{P} \to \emptyset \textit{ at rate } \beta.
\end{aligned}$$

Then, the average amount of protein in a population follows the differential equation

$$\frac{\mathrm{d}}{\mathrm{d}t} \langle x_p(t) \rangle = \mathsf{P}(\mathbf{X}(t)|_{\mathsf{D}} \in \mathsf{D}_1)\alpha - \beta \langle x_p(t) \rangle, \tag{2}$$

where $\langle x_p(t) \rangle$ denotes the average amount of the protein molecules at time t, and process $\mathbf{X}(t)|_{\mathsf{D}}$ is the projection of process $\mathbf{X}(t)$ to states at the promoter, that is $\mathbf{X}(t)|_{\mathsf{D}} = d$ if and only if $(\mathbf{X}(t) \in \cup_{i\geq 0}(d, i))$. In other words, $\mathsf{P}(\mathbf{X}(t)|_{\mathsf{D}} \in \mathsf{D}_1)$ denotes the marginal probability that the promoter is in active state (bound RNAP*) at time t.*

The proof is discussed in Appendix, Section 9. For an analytic derivation of further statistics of coupled promoter-state and protein copy-number (including how transient mean and noise depends on the covariance between the gene state and protein copy number, and the covariance matrix of the gene state with itself), we refer the interested reader to [22].

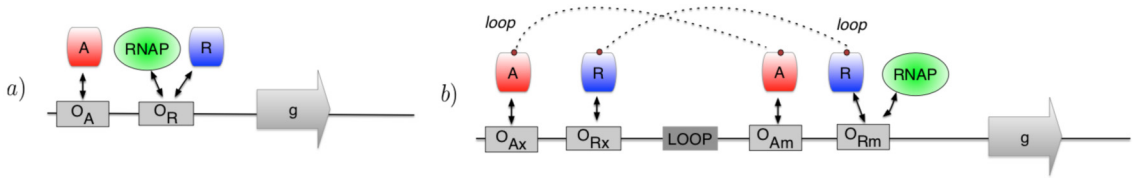

Fig. 3. Two prototype GRNs and their promoter logic: a) Model without looping: regulatory architecture (promoter logic), b) Model with looping: regulatory architecture (promoter logic). Mechanistic models are listed in (Appendix 8).

Corollary 1. *Assume that all reactions at the DNA are reversible, and that $\beta > 0$. Then, the probability of active promoter at stationarity, i.e., $\pi_1 = \lim_{t\to\infty} \mathsf{P}(\mathbf{X}(t)|_{\mathsf{D}} \in \mathsf{D}_1)$ exists, it is unique and will be converged to from any initial distribution [26]. Moreover, since $\beta > 0$, the system in Eq. (2) is asymptotically stable, and hence the average protein expression at the steady-state will not depend on its initial amount, nor on the initial distribution among the configurations of the DNA (Fig. 2 left), that is,*

$$\lim_{t\to\infty} \langle x_p(t)\rangle = \lim_{t\to\infty} \mathsf{P}(\mathbf{X}(t)|_{\mathsf{D}} \in \mathsf{D}_1)\frac{\alpha}{\beta} = \pi_1 \frac{\alpha}{\beta}. \tag{3}$$

In context of a circuit view, where TFs are inputs and population average of protein output, Corollary 1 suggests that perturbing the timing of inputs will not influence the protein amount at the steady-state, as long as the total quantities of input TFs are not altered.

When the DNA is modelled with one binding site, the promoter can be in only two states, and the analytic solution to Eq. (2) is tractable. In general, as activators and repressors bind to different regions (operator sites) of the same DNA molecule, the respective number of regulatory configurations at the promoter grows combinatorially with the number of operator sites. For instance, the mechanism that underlies the genetic switch of bacteriophage lambda, that contains three left and three right operators for the CI protein in the left and right promoters (PL and PR), leads to 1200 different DNA-TF configurations [8][1]!

In such cases, the simplification based on the argument of fast equilibrium is often employed, meaning that the transient protein dynamics is computed according to Eq. (3), thus neglecting the transient changes in probability distribution among the DNA regulatory configurations.

Fast equilibrium assumption is a prerequisite to applying a widely popular *statistical thermodynamics* model [27]. Assuming that the DNA regulatory configurations mix rapidly, this model allows to experimentally estimate the free energies of each promoter configuration, and then, subsequently, to derive the equilibrium constants[2] for each of the reactions [27,19]. As the absolute and precise values of kinetic rates are rarely available in practice, this method is powerful, because it allows to predict the dynamics of a genetic circuit from available experimental data. However, the statistical thermodynamics model is applicable only when the assumption of rapid equilibrium at the promoter is valid.

3. Searching for long lived transients

We focus on gene regulation without feedback, where activators and repressors are inputs, and the average protein expression in a population is the output. Assuming that a fixed amount of activators and repressors are added to the system with a possible time lag, our reference scenarios are the following (Fig. 11):

- $\mathcal{X}_{A||R}$ in which activator and repressor are introduced together,
- $\mathcal{X}_{A\to R}(\Delta)$ in which the activator is introduced Δ time units before the repressor, and
- $\mathcal{X}_{R\to A}(\Delta)$ in which the repressor is introduced Δ time units before the activator.

Our goal is to construct a genetic circuit with the following requirements: (i) it is realistic, that is - experimentally implementable in the sense that the mechanism can be implemented by the current technology and kinetic rate values are in realistic ranges, (ii) the scenarios provide striking differences in the shape and duration of transient protein output.

3.1. Prototype circuit

In this Subsection, we first describe the prototype circuit and show its desired behaviour of long lived transients. Then, in Section 4 and Section 5, we clarify this choice from point of view of the underlying dynamical system. Further biological details about the looping mechanism are given in the Supplementary material.

[1] Models used in this paper will count 23 and 6 distinct DNA binding configurations.
[2] The ratio between the binding and unbinding rate.

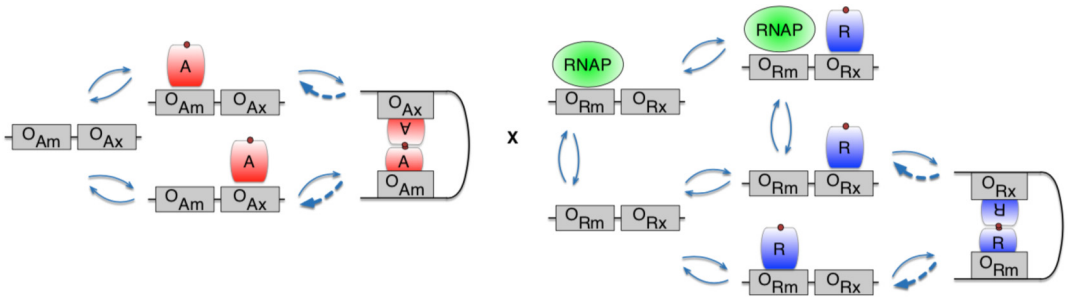

Fig. 4. Model with looping: CTMC regulating the DNA configurations has 23 different states. It is naturally represented as a composition of two sub-models: (left) the switching among configurations with respect to activator binding to its main and auxiliary binding sites (O_{Am} and O_{Ax} respectively), and (right) the switching among configurations with respect to repressor binding to its main and auxiliary binding sites (O_{Am} and O_{Ax} respectively). The unlooping rates (dashed blue lines) are typically much lower than the unbinding of a single TF. Any combination of the states in the two sub-models is is reachable, except the state where both repressor and activator are looped. The mechanism is encoded in a rule-based modelling language, with twenty five rules for the model with looping, which would require more than 130 reactions to specify an equivalent mechanism with reaction-lists. For further details, we refer the reader to the full model shown in the Supplementary material.

Model with looping. Our prototype circuit with DNA looping mechanism is inspired by the very well-characterised regulatory mechanisms of the *lac* operon and of the bacteriophage lambda genetic switch [28,29]. In the model with looping (Fig. 3, right), two activators and two repressors can bind the DNA; Binding of the second activator (resp. repressor) promotes looping of the DNA in the active (resp. repressed) state, thereby excluding binding of the other TF. For this reason, all states except the state where both active looped and repressed looped state will be reachable. For further details, we refer the reader to the rule-based model in the Supplementary material.

Implementation. We mechanistically model the reactions at the promoter, and the combinatorial blow-up of states at the DNA. Models are written and analysed within the rule-based modelling framework Kappa, a domain-specific language for modelling biochemical reactions. Kappa allows to naturally encodes the information processing at the DNA, uses wildcard symbols to make the description compact (e.g. twenty five rules for the model with looping, which would require more than 130 reactions to specify an equivalent model), and supports an efficient stochastic simulation algorithm [30,31]. Source-code of the rule-based models is given in Section 8. Parameter exploration and additional output analysis were performed with Python.

Model without looping. For reference, we also analyse a simpler model without the looping mechanism (Fig. 3, left). A basic mechanism for activation and repression is assumed: repressor R competes with RNAP, and the activator A recruits the polymerase RNAP and binds independently of the repressor and the polymerase (configurations shown in Fig. 12).

Simulation. We simulated multiple samples of the stochastic model, and we statistically estimated the average protein expression. In the model with looping, we used 1000 individual cells for a time of 36000s = 10 h, which equals around 20 average cell doubling times, where inputs are added from time point $t_0 = 5400 = 1.5$ h (see Table 2 for all simulation parameters).

Kinetic rates. All model parameters are in realistic ranges taken from the literature, given in Table 1 and further explained in the Appendix. The mechanism for the activator is inspired by the λ-phage. The mechanism for repressor is inspired by the lac operon. Further values that were tested to show the generality of our approach came from other well-characterised TFs such as CRP. The chosen parameter values were found in the literature, both for the scenario without looping [32,33] and for the scenario with looping [34–38].

Cell division. We do not explicitly model the event of cell division, and the respective distribution of the cellular material and potentially associated events of unlooping or unbinding of TFs. In our model, division is implicitly incorporated in the protein decay rate, and we assume that at once input, activators and repressors remain constant.

Parameter search. We implemented a grid search of the viable parameter space (for different levels of eleven kinetic rate parameters, and the amounts of activator, repressor and RNAP), where we compute the average protein expression, amplitude and half-life for a subset of all parameter combinations. In our implementation, the user specifies a range for each parameter, and the models are executed, figures drawn for each possible parameter combination.

Quantitative characteristics of long lived transients. To quantify the long lived transients, we will use two quantitative measures:

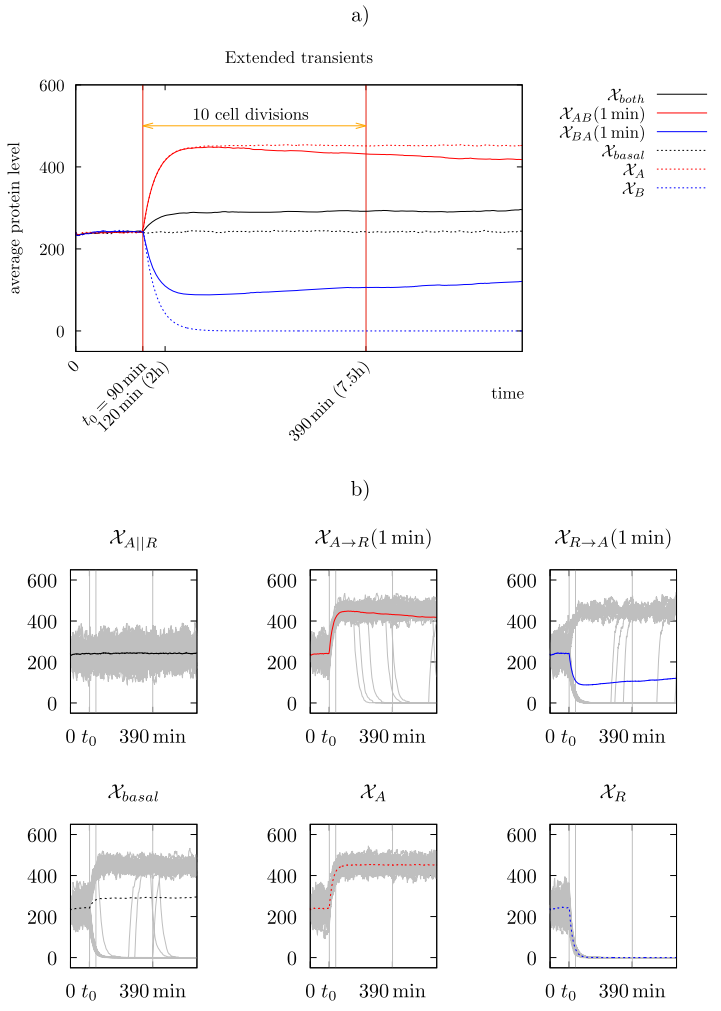

Fig. 5. A small delay in arrival times of TFs can give rise to qualitatively opposite, stable transient phenotypes for a long period of time. a) Average protein level for a population of 1000 cells, in three input scenarios (full lines) and three reference scenarios (dotted lines). b) 50 single cell traces (grey lines) and the respective average, for each of the six modes.

- *amplitude*, the maximum distance in phenotype of the scenario with delay from the scenario without delay, that is

$$\alpha_{|s} := \max_{t \geq t_0} |\langle x_p \rangle(t|s) - \langle x_p \rangle(t|\mathcal{X}_{A||R})|,$$

  where s refers to the scenario in question ($\mathcal{X}_{A\to R}(\Delta)$ or $\mathcal{X}_{R\to A}(\Delta)$) and $x_p(t|s)$ denotes the average protein number in a population at time t in scenario s, and
- *halflife*, the time the system takes from the moment of reaching the amplitude, to the moment when the distance from the phenotype without delay is half-way, that is

$$t_{1/2|s} := \arg\min_{t \geq t_{\alpha|s}} \{t \mid |\langle x_p \rangle(t|s) - x_p(t \mid \mathcal{X}_{A||R})| < \frac{1}{2}\alpha_{|s}\},$$

  where $t_{\alpha|s}$ denotes the moment when the amplitude is reached in scenario s.

In summary, the *amplitude* reflects how observable is the sensitivity to the delay among inputs, and the second measure, *halflife*, reflects how slow is the convergence to the real equilibrium after the amplitude has been observed. We call a phenotype a *long lived transient*, if it is characterised by a large amplitude, and an extended half-life. The notion of 'large' and 'extended' should be interpreted wrt. the observational scale: amplitude should be seen as qualitatively distinct for the experimental system at hand, and, the half-life should be so long, that the gradient of the transient from the point of amplitude to the point of observation appears to be zero. Time of observation is a duration of an experiment, which is typically of order of cell doubling time. Further, formal quantification of long lived transients is out of scope of this manuscript and we leave it to future work.

4. Results

In further text, by *phenotype*, we mean the average protein expression in a population of 1000 cells. Recall from Corollary 1, that all three scenarios $\mathcal{X}_{A||R}$, $\mathcal{X}_{A\to R}(\Delta)$ and $\mathcal{X}_{R\to A}(\Delta)$ converge to the same phenotype. As a reference, we also analyse the scenarios where no TFs are input ($\mathcal{X}_{basal}$), only activators ($\mathcal{X}_A$) or only repressors are input ($\mathcal{X}_R$). We investigated the phenotype in the three scenarios for a large range of parameter combinations. (There are $2^{11} > 2000$ combinations when only two values for each parameter are set.) We choose one parameter set as the *reference parameter set* (shown in Fig. 5a), where the phenotypes are symmetric with respect to the $\mathcal{X}_{A||R}$ scenarios in the sense that the protein expression deviates in the same amount from the phenotype of $\mathcal{X}_{A||R}$ and the rate of reaching the phenotype of $\mathcal{X}_{R||A}$ is of the same scale.

1 A small delay in arrival times of TFs can give rise to qualitatively opposite, stable transient phenotypes for a long period of time. In Fig. 5a, we plot the observable phenotype – the mean of protein expression for a given population of cells – in the three regimes of interest (full lines) and the three reference regimes (dotted lines). Three distinct transient phenotypes are observed: the transient for the input $\mathcal{X}_{A||R}$ lasts roughly for one average cell doubling time (30 min), while both phenotypes for $\mathcal{X}_{A\to R}(1\,\text{min})$ and $\mathcal{X}_{R\to A}(1\,\text{min})$ last well over 10 average doubling times.

In Fig. 5b, we see that the response of individual cells is bimodal: they exhibit 'all-or-none' behaviour, having high or low expression and the phenotype depends on whether the cell entered the active looped state or the repressed looped state. The expected time that a cell spends in one looped state is long. To illustrate this, we display the protein expression for 50 randomly chosen single cells is displayed in Fig. 5b for each of the three regimes. In regime $\mathcal{X}_{A||R}$, an individual cell either has high expression at around 400 proteins or low expression, being fully inhibited. The noise around the low expression value is not observable in the plot, because when the promoter is in the repressed looped state, protein expression is fully inhibited. If the DNA unloops and subsequently loops towards a different regulatory state, e.g. from looped repressed to looped active state (or vice-versa), the protein expression will change from low to high expression (or vice-versa). In the taken time window (10 hours), three (out of 50) displayed traces switching from the high to low expression level and one trace switching from low to high expression level. The average expression in a given population (thick line in respective colour) is saturated at around 270 protein molecules. In regime $\mathcal{X}_{A\to R}$, all of the displayed 50 cells enter the active looped state before the repressors are input, but, due to the slow unlooping, the high expression profile is long-preserved, resulting in slow switching towards the low-expression state, and hence long transient time towards the average expression. In regime $\mathcal{X}_{R\to A}$, even though repressors are input first, some cells activate expression, but in most cells, expression is first inhibited. Similarly as in the profile $\mathcal{X}_{A\to R}$, since DNA unlooping from the repressed state is slow, the transient of the average protein expression is also slow. The reference scenarios - $\mathcal{X}_{basal}$, $\mathcal{X}_A$ and $\mathcal{X}_R$ show the expected behaviour.

Recall that, in our model, division is implicitly incorporated in the protein decay rate, and we assume that at once input, activators and repressors remain constant. To this end, the validity of our model after the cell division may be questioned. Yet, even if our model is valid only up to a small number of cell division cycles (we indicate 10 division cycles in Fig. 5), our main argument holds: the prototype circuit exhibits qualitatively distinct phenotypes, which appear to be stationary, and occur due to small delays in input.

2 Parameter sensitivity. Are long lived transients a consequence of system regulatory architecture or a careful tuning of kinetic parameters? We chose six different parameter combinations, listed in Table 1, and we reproduce the plot shown in Fig. 5a for each of the parameter combinations, each for three time delays - 1 min, 5 min and 15 min. $\mathbf{p}_1$ is the reference parameter set (the plot shown in Fig. 5). Results confirm that the long lived transients are preserved with the chosen parameter changes. Higher unlooping rate for either activators or repressors results in shortening the transient and moving the average expression level to lower and higher value respectively ($\mathbf{p}_2$ and $\mathbf{p}_3$). While decreasing the number of activators does not change the phenotype much ($\mathbf{p}_4$), decreasing the number of repressors results in complete dominance of activation effect when both TFs are input simultaneously ($\mathbf{p}_5$). Still, the delay of activator input shows full repression profile for a long period of time. When RNAP rates are scaled so that the binding and unbinding rates are both ten times slower, the duration of transients shortens and the three input regimes show the same output after much shorter time ($\approx$10 hours, $\mathbf{p}_6$). While local sensitivity analysis gives an idea about how individual parameters affect the phenotype, a systematic sensitivity analysis of this model is out of scope of this paper, and we leave it to future work.

In Fig. 8 (up, model with looping), we see that the reference parameter set ($\mathbf{p}_1$) has a halflife longer than 20 hours no matter if the delay occurs in favour of the activator or repressor. The halflife decreases significantly in cases when the unlooping rate is decreased (one at a time - $\mathbf{p}_2$ and $\mathbf{p}_3$), or when RNAP binding and unbinding rate is scaled down ($\mathbf{p}_6$), while the change in the number of activators/repressors reflect more on the amplitude than on the halflife ($\mathbf{p}_4$, $\mathbf{p}_5$).

3 Long lived transients are not observed in the model without looping. We next inquire how changes in regulatory architecture affect the behaviour, i.e. is DNA looping essential for observing the long lived transients? We repeated the experiments on a model without looping. Phenotypes for six parameter combinations, listed in Table 1,[3] are each studied for three time

[3] Notice that these six parameter combinations are different than those used for the model with looping.

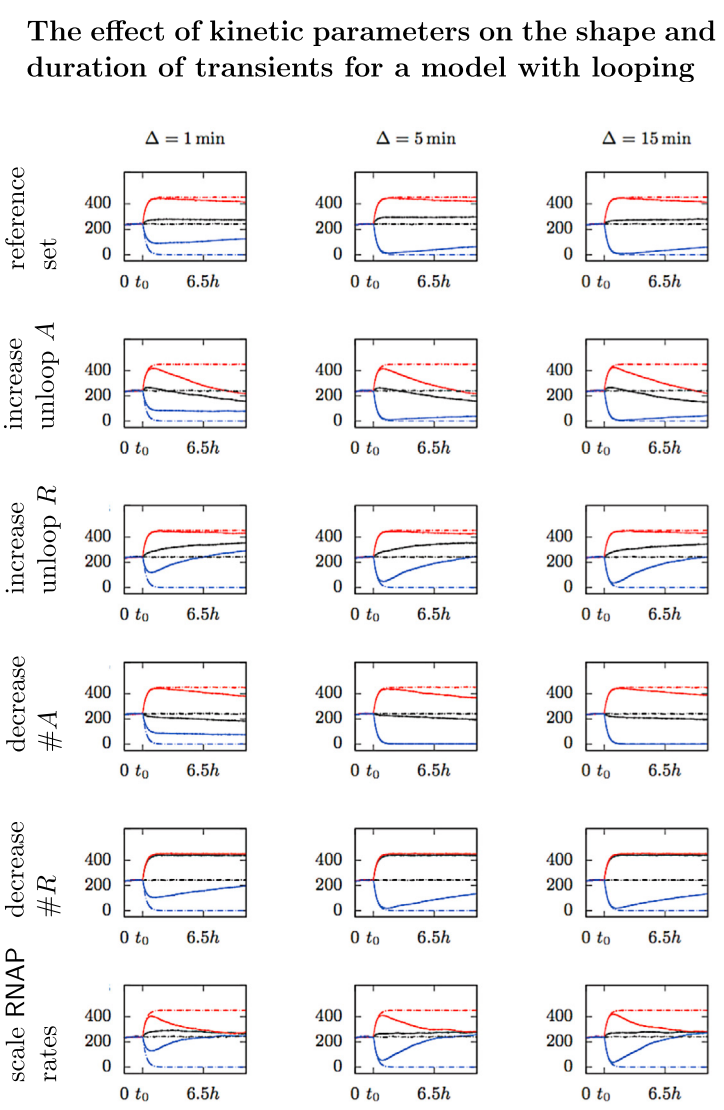

Fig. 6. The effect of kinetic parameters on the shape and duration of transients for a model with looping (for six parameter values listed in Table 1 and time delays of 1 min, 5 min and 15 min respectively).

delays (Fig. 7). For all parameter combinations, the amplitude and duration of transient regimes is clearly correlated with the duration of delay - the longer delays induce longer transient regimes. The transient phase is significantly shorter than in the model with looping (notice the different time-scale than in Fig. 5 and Fig. 6), but they still can last for several cell doubling times (for delays of 15 min up to 2.5 h or 5 average doubling times). However, they are not long lived transients, as the shape of transients clearly reveals that the steady-state regime is going to be reached later on, that is, the transients in this model would not be easily confused with the steady state. The observations above are indicating that looping is essential for creating the effect of long lived transients. $\mathbf{p}_1$ is the reference parameter set, which we choose so that the level of expression when both activators and repressors are input is close to basal (the TFs neutralise each-other's effect overall). As expected, decreasing the recruitment by the activator results in lower stationary expression ($\mathbf{p}_2$), increasing the number of repressors results in stronger repression ($\mathbf{p}_3$), weakening the repressor binding results in higher expression ($\mathbf{p}_4$), weak binding of repressor in combination is not affected by decreasing the recruitment by activator simultaneously ($\mathbf{p}_5$) and weak binding of repressor in combination with more repressor molecules results in low expression ($\mathbf{p}_6$).

In the summary of characteristics of long lived transients for the model without looping (shown in Fig. 8 down), we see that, for a delay of 5 min, all parameter combinations achieve the amplitude at comparable scale as that in the case of model with looping. However, the maximal halflife in all tested parameter points is 15 min, a 100-fold difference with respect to the halflife of long lived transients in the model with looping, confirming that adding the looped configurations was essential for the effect of long lived transients.

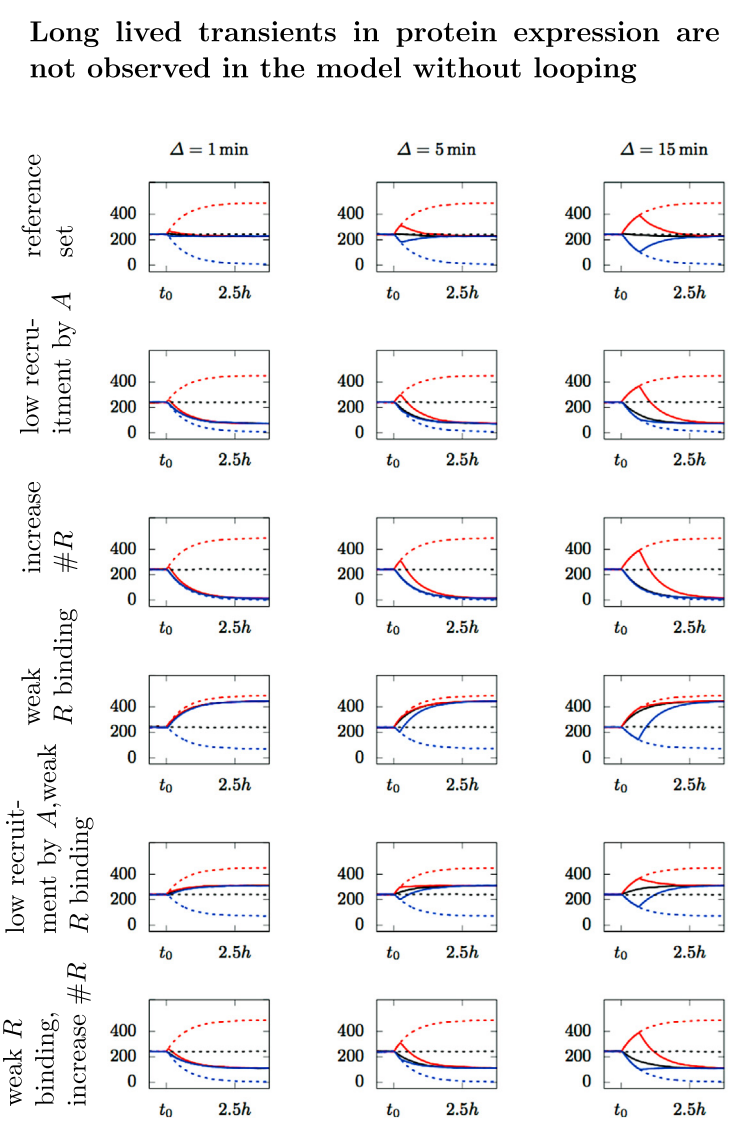

Fig. 7. The effect of kinetic parameters on the shape and duration of transients for a model with looping (for six parameter values listed in Table 1 and time delays of 1 min, 5 min and 15 min respectively).

4 Phenotypes in long lived transients can be modulated by the delay between inputs. We now comment on the dependency on the delay. In Fig. 9, the phenotypes in scenario $\mathcal{X}_{A\to R}(\Delta)$ are observably equivalent for all chosen values of delay. In particular, they transiently reach the same protein expression value as the scenario $\mathcal{X}_A$ where only activator is present. Therefore, this scenario seems to be independent of delay timing between TFs as long as the delay occurs in favour of the activator. On the other hand, the difference between phenotypes in scenario $\mathcal{X}_{R\to A}(\Delta)$ is different for delay $\Delta = 1\,\text{min}$ than for delays $\Delta \in \{5\,\text{min}, 15\,\text{min}\}$. While for all three delays, the effect of long lived transients can be observed (the slope of approaching the limit value is small), the phenotype (protein expression around which the transients seem to stabilise) is different. It appears that, unlike delays longer than 5 min, the delay of 1 min is not long enough for the population to repress protein expression to a value as low as in the scenario $\mathcal{X}_R$ (where only repressor is present). In other words, the lowest gene expression value for delay of 1 min is never as small as in the scenario $\mathcal{X}_R$. To investigate the dependency of the transient phenotype on the delay, we simulated the scenario for several delay values between 1s and 5 min, namely $\Delta \in \{1\text{s}, 20\text{s}, 40\text{s}, 60\text{s}, 120\text{s}, 180\text{s}\}$ and we computed the amplitude for the scenario $\mathcal{X}_{R\to A}$. The plot in Fig. 9 demonstrates that the amplitude approaches the value of $\mathcal{X}_R$ scenario exponentially fast with increasing delay time.

Plotting the phenotypes for scenario $\mathcal{X}_{A\to R}(\Delta)$ for delays between 1s and 1 min shows that the same activated gene expression levels are observed even for delays as small as 1s (plots not shown). The explanation for different sensitivity of transient phenotypes to the delay in scenarios $\mathcal{X}_{A\to R}(\Delta)$ and $\mathcal{X}_{R\to A}(\Delta)$ are the different mechanisms implementing the activation and repression. When activator is input first, it quickly binds both operator sites and the probability of being in the looped active state almost instantaneously increases to the maximum value (as fast as within 1s), and then starts

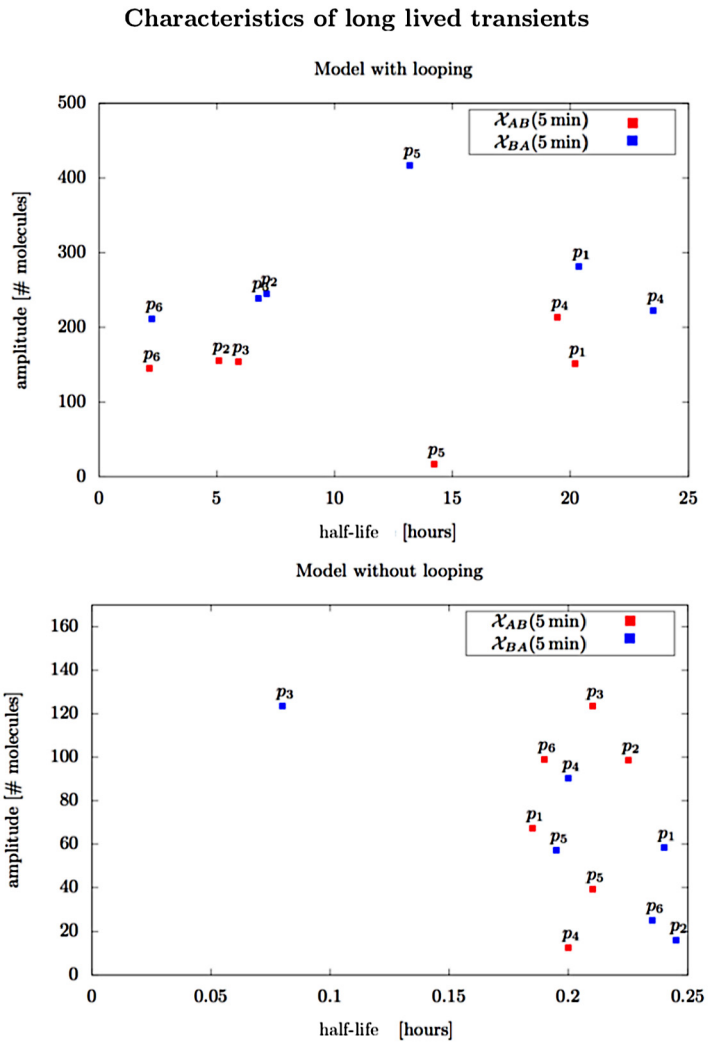

Fig. 8. For chosen parameter sets (Table 1 and Table 1) and for a delay $\Delta = 5$ min, we plot the amplitude and the half-life (defined in Sec. 4). Observe that the time-scales differ 100-fold.

decreasing only very slowly towards the equilibrium as soon as the repressor is present as well. On the other hand, when the repressor is input first, it does not bind both operator sites as quickly, because it is competing with the abundant RNAP, even while the activator is not in the system. Only if there is enough time for the repressor to reach the looped repressed state with a probability nearly as high as in case of repressors only, the maximally repressed expression level will be observable. Otherwise, as soon as the activator is in the system, the probability of being in the looped repressed state starts shifting slowly towards the equilibrium point, and, consequently, the protein expression in the population starts increasing.

5. Towards a mechanistic characterisation of long lived transients

The CTMC for the DNA switching of our prototype circuit with looping is inspired by the very well-characterised regulatory mechanisms of the *lac* operon and of the bacteriophage lambda genetic switch [28,29]. We next ask in which general promoter architectures we expect to observe long lived transients.

Networks of DNA configurations. We aim to describe a generic network structure of the CTMC among the DNA states regulating a single protein without feedback. In Fig. 10a), we depict a central state where no regulatory molecules are bound to targets at the DNA by d_0, and states that can be reached with $i \geq 1$ successive binding reactions are indexed by i $(d_i, d_i', d_i'', \ldots)$. Due to the reversibility of all reactions at the promoter, each configuration is reachable from another one. Reaching one configuration from another is typically possible through different paths of reactions (e.g. activator binding and RNAP binding can happen in any order). However, some reactions may prevent the subsequent application of others,

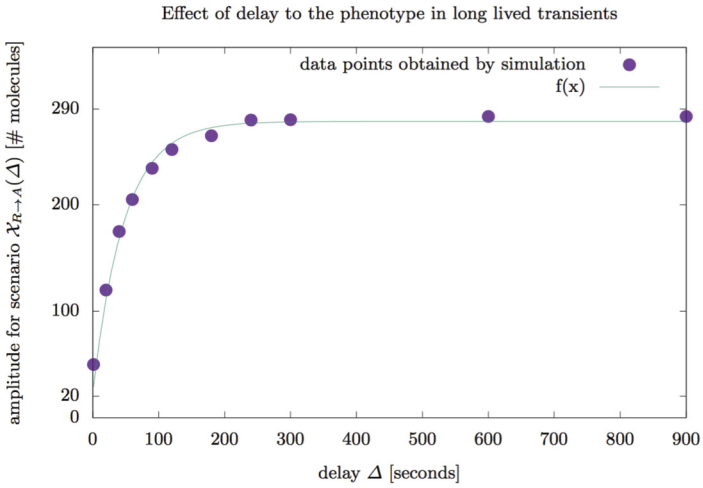

Fig. 9. In the reference parameter set, when there is no delay ($\Delta = 0$), the phenotype in scenario $\mathcal{X}_{R\to A}(\Delta)$ is equal to the one in scenario $\mathcal{X}_{A||R}$, visibly different than the phenotype $\mathcal{X}_R$ (290 protein molecules). The difference from the scenario $\mathcal{X}_{A||R}$ (the characteristic we formally termed *amplitude* – see Section 4) exponentially grows as the delay increases, that is, it quickly approaches the phenotype of scenario $\mathcal{X}_R$. The difference of $\mathcal{X}_{R\to A}(\Delta)$ from $\mathcal{X}_R$ becomes observably negligible already for delays larger than $\Delta = 5\,\text{min} = 300\text{s}$ (difference of 10 molecules, 0.035% of the initial difference). We obtained the dependency by fitting the data obtained by simulating the system for $\Delta \in \{1, 20, 40, 60, 120, 180, 240, 300, 600, 900\}$.

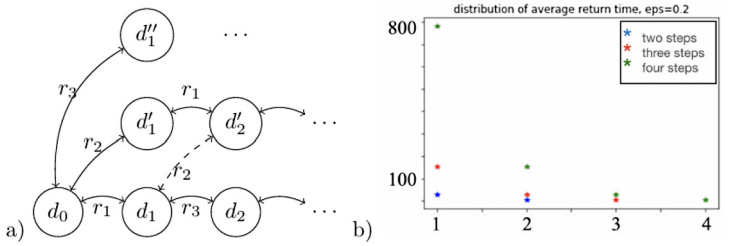

Fig. 10. a) A generic CTMC among promoter states: an empty DNA where no regulatory molecules are bound to respective targets (state d_0) can transition to another DNA state in one, two, or a finite number of ordered reaction events, occurring at possibly different time-scale. Sometimes, an intermediate state can return towards state d_0 through several different reactions (e.g. state d_2'), and equally fast as others. Alternatively, it is possible that there is only a single or a few reactions leading back towards d_0 (e.g. state d_2), and that some of these reactions are much slower than others. The existence of such states will increase the average return time to d_0, and respectively time to equilibration of the overall chain. b). Illustration of Lemma 2: In the extreme case of fully independent branches of length K, with only fast forward reactions (at rate equal to 1) and slow backward reactions (at rate $\varepsilon < 1$), the average return time at state d_0 grows exponentially in K. We illustrate the distribution of average return times, for $\varepsilon = 0.2$ and chain length varying from one to four.

typically when acting over overlapping promoter regions (such as inhibitor and RNAP competing to bind at the same region of DNA). Hence, the network of DNA configuration will not be complete, and transitions will typically exist between states indexed with close-by values. Moreover, it is also important to account for the relative magnitudes of reaction propensities, i.e. weights in this network. The distribution of the weight magnitudes can be considered uniform at random, in the context of representation in Fig. 10.

Prolonging the transients. In general, a chain equilibrates after it is well-mixed, i.e. each of its states has been visited sufficiently often, so that new transitions do not affect the distribution of probability mass. Markov chain *mixing time* is formalised as the time it takes to be ϵ-close to equilibrium across all states. Mixing time depends on the initial distribution, the chain connectivity, and the rate parameters. In particular, long mixing times are prominent for chains with a large spectral gap of the underlying generator matrix, and, as a consequence, can be guaranteed for chains with large connectivity diameter, suggesting that more states and sparse connectivities generally can prolong the mixing time.

Tightly estimating bounds on the mixing time for any given chain remains a challenge [39]. We instead point to instances of network in Fig. 10 where reaching one configuration from another requires a unique slow reaction to occur. In particular, when communication between states in different branches is possible only via states close to d_0, and when all binding reactions are fast relative to unbinding ones, the expected return time increases exponentially with the length of the complexion steps.

Lemma 2. *For a generic CTMC depicted in Fig. 10, assume that all outgoing rates from state d_0 sum to 1, and that each forward and backward reaction rate between states d_i and d_{i+1}' equal 1 (fast) and ε (slow) respectively. Assume that there is no communication*

between states, except from via d_0, and that each branch has length $K \geq 1$. Then, the average return time to d_0 equals $(\frac{1}{\varepsilon})^K(1+\varepsilon+\ldots+\varepsilon^K)$.

Proof 1. After lumping the behaviourally equivalent pairs of states $\{d_i, d_i', \ldots\}$, $i = 1, \ldots, K$ [40], the quotient chain is a queueing system of type M/M/1/K (single server, limited buffer, for $\lambda = 1$ and $\mu = \varepsilon$). The stationary distribution for K buffer states and parameters λ and μ equals $\pi_i = \rho^i \frac{1-\rho}{1-\rho^{K+1}}$ where $\rho = \lambda/\mu$ [41]. The average return time is inversely proportional to its stationary distribution, hence the result follows by applying the general formula to state d_0.

The Lemma shows that, in general, when reverse reactions are on a slow time-scale, the average return time to state d_0 can be exponentially amplified with the length of the specific path to the largest formed complex. Assume now that there are biophysical limits to the absolute values of reaction rates, e.g. ranging between ε and 1. Our observation implies that, when extending the transients is not possible via lowering the reaction rates, it is possible by adding new DNA configurations. For example, if the maximum expected return time for $K = 1$ is $\frac{1}{\varepsilon}(1+\varepsilon)$, the maximum return for $K = 2$ is $\frac{1}{\varepsilon^2}(1+\varepsilon+\varepsilon^2)$ (concrete instantiations are illustrated in Fig. 10b).

'Slow-by-fast' transients. In summary, our insights confirm that DNA looping architecture inducing a CTMC with 23 states was a good candidate for creating long mixing times, because the looped states are hard to exit relative to other states, and their specific complexation path counts several reactions. One other such instance of Fig. 10a), with only four-states,[4] was shown to exhibit a related phenomenon called 'slow-by-fast' transients [22]. Namely, in the general case of any promoter network, and in agreement with the rapid equilibrium assumptions, it is expected that increasing all reaction rates speeds up the transient expression and reduces the protein noise. However, using a special case of the network Fig. 10a) with only four states, [22] shows that, counter-intuitively, accelerating reactions at the promoter non-uniformly can slow down transient gene expression and keep the noise level unreduced.

6. Discussion

Given that the processes of transcription and translation of a gene into a protein introduce intrinsic time delays and that there is no global synchronisation among the arrival times of different molecular species at molecular targets, the simultaneous arrival of TFs in genetic circuits is a strong assumption. We subjected this assumption to a perturbation analysis, where the perturbed parameters are the relative arrival times of the TFs (different to the usual choices of perturbation parameters being the kinetic rates). We simulated a simple and realistic genetic circuit with two inputs and we showed that, in presence of small perturbations in the arrival of inputs (shorter than 1 min), the circuit can exhibit three qualitatively distinct phenotypes which are stable for as long as any typical experiment would last (longer than 20 cell doubling-times). This has wide implications.

First, while our showcase example was constructed with the goal of demonstrating that long lived transients can appear in gene regulation, there are reasons to believe that many other gene regulatory schemes also exhibit long lived transients and implement multiple phenotypes by modulating the timing of inputs. To see this, consider that the number of potential phenotypes grows factorially with the number of inputs per gene as it is determined by the number of possible input orderings, meaning that, for instance, only 5 inputs would require us to analyse 5! = 120 different input scenarios. Moreover, our analysis indicates that long lived transients are possible in promoters with many configurations and certain states that are easy to reach but hard to exit. For instance, genomic regulation of the development of sea urchin embryo shows potential for long lived transients. The relevance of transient TF production has already been determined in this system [42,43]: multiple TFs regulate a single gene which in turn has multiple targets, and there is clear differentiation between upstream and downstream components in the network. Therefore, considering long lived transients might clear up some puzzling observations like the discrepancy of TF interactions between endogenous promoters and minimal promoters controlled by three Endo16 regulatory modules [44].

Secondly, our proof-of-concept case study suggests that any modelling approach which assumes perfectly synchronous arrival of TFs or assumes rapid equilibrium at the promoter, may fail to explain a variety of phenotypes and raise false conclusions. To illustrate this point, think of an experimentalist who observes the system which seems equilibrated, but is a long lived transient (e.g. in our case study, a delay in favour of the activator occurs). Assuming that what is seen is an equilibrium, following the approach of statistical thermodynamics, one would proceed by estimating the free energies of binding configurations, but these estimates would be wrong, as the real equilibrium is much further away. Moreover, the obtained model would explain a single phenotype, and not the variety of quasi-stable phenotypes such as the ones we see in our showcase example. In summary, one cannot ignore the order of stimulating a cell, even when the GRN under consideration is assumed to be feedback-free. Similarly, one cannot assume what is observed towards the end of the life cycle is close to equilibrium even when the system seems relatively stable, e.g. growth at steady state in bulk, even when the stimulation was completed very early on. For distinguishing between a long lived transient and a real equilibrium, it

[4] The four-state chain used in [22] can be seen as an abstraction of our 23-state chain of the model with looping Fig. 4.

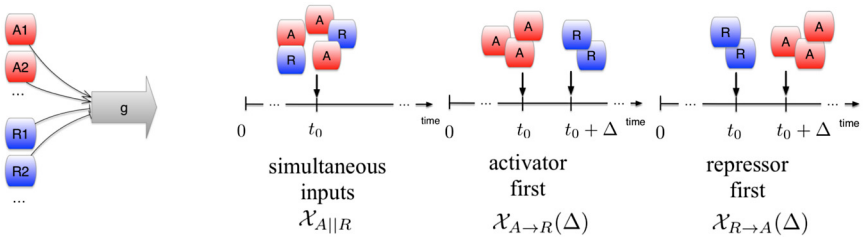

Fig. 11. Searching for long lived transients in gene regulation without feedback: three modelled scenarios. We demonstrate that small delays Δ can raise qualitatively different phenotypes, which are stable for cell lifetime.

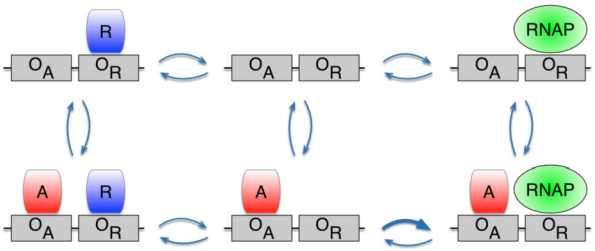

Fig. 12. Model without looping: the CTMC regulating six different DNA configurations. Thicker blue line denotes that the recruitment of RNAP is faster when the activator is bound.

becomes of critical importance to write down detailed mechanistic models, experimentally measure the kinetic rates as accurately as possible, and to take the timing of inputs into account. To this end, the key challenges for future work are automated and efficient algorithms and tools for performing the parameter search, which will support the detection of long lived transients 'in vivo'.

Finally, our case study opens the possibility that GRNs are exploiting event timing to perform desired behaviours - it suggests that the cell does not necessarily compute with equilibrium dynamics - as is widely assumed in the field (with the exception of 'well behaved' limit cycle behaviours or pulsatile behaviour [45]), but uses the transients to react to stimuli and to memorise events. The DNA may be encoding more phenotypes in reference to what the conventional input to output mapping suggests. In particular, as our analysis of delay timing between TFs shows (Fig. 9), a whole range of different stable gene expression levels can be encoded in the event timing of inputs. More broadly, this aspect may provide an explanation to why an organism can display so many more phenotypes, though the number of genes is limited, as the complexity of the organism increases, e.g. number of genes in bacteria and human vary by a factor of only 4!

Related work. Given that the next goal of synthetic biology is to build composable systems of increasing complexity, timing aspects of gene regulation are increasingly gaining attention. The consequences of combined effects of time delay and intrinsic noise on gene regulation has been studied in [46]. In [47], the authors elucidate the importance of relative timing of TF activation in combinatorial gene regulation with pulsatile signals. Like Lin et al. [47], our work shows that relative timing between TFs may be used by the cell to implement responses to different environments and therefore has to be taken into consideration for modelling gene expression patterns. However, while the authors in [47] suggest that the phenotypes differ in pulsatile regulation patterns, our study reveals the existence of long lived transients. From a dynamical system point of view, the effect of long lived transients that we present here can be seen through the prism of general theoretical frameworks such as proposed in [48–50], where the authors discuss how to detect and automatically compute the meta-stable states from only the topology and timescales of the network; Other works include explicitly modelling delays in gene expression [51], resolving the temporal dynamics of gene regulatory networks from time-series data [52], examining the relation between topology and relaxation to steady states of reaction networks [53], as well as the study of transient hysteresis and inherent stochasticity in gene regulatory networks [54]. It would be interesting to see how precisely these methods could be used to detect the long lived transients we showcase in this paper.

Of relevance for synthetic biology, our construction based on looping suggests a way to implement memory units, though they may be leaky, in the sense that the signal is slowly being lost. In a broader context, cellular memory refers to systems whose present phenotype is dependent on the history of input stimuli and therefore the trajectory by which it has been reached [55]. The molecular mechanisms associated with such memory effects are usually based on feedback loops (e.g. the E. coli lac operon), DNA methylation patterns (e.g. temperate phage, pilus synthesis, cell differentiation) or inversions catalysed by site-specific recombinases (e.g. the Salmonella Hin system or the E. coli Fim system) [55,56]. The long lived transient behaviour observed in our simulations differs from the mentioned memory mechanisms as it is purely relying on dynamical stability of the transcriptional state. Different to the usual references to cellular memory, the long lived transients require no stabilisation of the phenotype through strong (covalent) modification of the DNA or any kind of feedback of the output on the promoter state (which is generally considered necessary for cellular memory).

The nature of the observed long lived transient states confer an epigenetic nature to these states. Methylation of histones is widely used in eukaryotic gene regulation as a modulator of gene activity that confers memory and stability to gene expression states. However, unlike methylation that requires a sleuth of specialised proteins that expend energy in order to form covalent bonds of methyl groups to histones, the long lived transients arise simply as a dynamical property of the system.

Declaration of competing interest

The authors declare that they have no known competing financial interests or personal relationships that could have appeared to influence the work reported in this paper.

Acknowledgements

Tatjana Petrov's research was supported in part by SNSF Advanced Postdoctoral Mobility Fellowship grant number P300P2 161067, the Ministry of Science, Research and the Arts of the state of Baden-Wurttemberg, and the DFG Centre of Excellence 2117 'Centre for the Advanced Study of Collective Behaviour' (ID: 422037984). Claudia Igler is the recipient of a DOC Fellowship of the Austrian Academy of Sciences. Thomas A. Henzinger's research was supported in part by the Austrian Science Fund (FWF) under grant Z211-N23 (Wittgenstein Award).

Appendix A. Supplementary material

Supplementary material related to this article can be found online at https://doi.org/10.1016/j.tcs.2021.05.023.

References

[1] H.H. McAdams, A. Arkin, It's a noisy business! Genetic regulation at the nano-molar scale, Trends Genet. 15 (2) (1999) 65–69.
[2] C.C. Guet, M.B. Elowitz, W. Hsing, S. Leibler, Combinatorial synthesis of genetic networks, Science 296 (5572) (2002) 1466–1470.
[3] M.A. Marchisio, J. Stelling, Automatic design of digital synthetic gene circuits, PLoS Comput. Biol. 7 (2) (2011) e1001083.
[4] T. Friedlander, R. Prizak, C.C. Guet, N.H. Barton, G. Tkačik, Intrinsic limits to gene regulation by global crosstalk, Nat. Commun. 7 (1) (2016) 1–12.
[5] F. Jacob, Evolution and tinkering, Science 196 (4295) (1977) 1161–1166.
[6] A. Nagy-Staron, K. Tomasek, C.C. Carter, E. Sonnleitner, B. Kavčič, T. Paixão, C.C. Guet, Local genetic context shapes the function of a gene regulatory network, eLife 10 (2021) e65993.
[7] R. Kwok, Five hard truths for synthetic biology, Nature 463 (7279) (2010) 288–290.
[8] M. Santillán, M.C. Mackey, Why the lysogenic state of phage λ is so stable: a mathematical modeling approach, Biophys. J. 86 (1) (2004) 75–84.
[9] E.A. Trofimenkoff, M.R. Roussel, Small binding-site clearance delays are not negligible in gene expression modeling, Math. Biosci. (2020) 108376.
[10] D. Gillespie, Exact stochastic simulation of coupled chemical reactions, J. Phys. Chem. 81 (1977) 2340–2361.
[11] T.G. Kurtz, Solutions of ordinary differential equations as limits of pure jump Markov processes, J. Appl. Probab. 7 (1) (1970) 49–58.
[12] L. Cardelli, M. Kwiatkowska, L. Laurenti, Stochastic analysis of chemical reaction networks using linear noise approximation, Biosystems 149 (2016) 26–33.
[13] J. Gunawardena, Time-scale separation–Michaelis and Menten's old idea, still bearing fruit, FEBS J. 281 (2) (2014) 473–488.
[14] S. Peleš, B. Munsky, M. Khammash, Reduction and solution of the chemical master equation using time scale separation and finite state projection, J. Chem. Phys. 125 (20) (2006) 204104.
[15] A. Beica, C.C. Guet, T. Petrov, Efficient reduction of kappa models by static inspection of the rule-set, in: International Workshop on Hybrid Systems Biology, Springer, 2015, pp. 173–191.
[16] R. Srivastava, E.L. Haseltine, E. Mastny, J.B. Rawlings, The stochastic quasi-steady-state assumption: reducing the model but not the noise, J. Chem. Phys. 134 (15) (2011) 154109.
[17] E. Segal, J. Widom, From DNA sequence to transcriptional behaviour: a quantitative approach, Nat. Rev. Genet. 10 (7) (2009) 443–456.
[18] L. Bintu, N.E. Buchler, H.G. Garcia, U. Gerland, T. Hwa, J. Kondev, T. Kuhlman, R. Phillips, Transcriptional regulation by the numbers: applications, Curr. Opin. Genet. Dev. 15 (2) (2005) 125–135.
[19] C.J. Myers, Engineering Genetic Circuits, CRC Press, 2009.
[20] C. Guet, T.A. Henzinger, C. Igler, T. Petrov, A. Sezgin, Transient memory in gene regulation, in: International Conference on Computational Methods in Systems Biology, 2019.
[21] R. Byers, R. Hansell, N. Madras, Stability-like properties of population models, Theor. Popul. Biol. 42 (1) (1992) 10–34.
[22] P. Bokes, J. Klein, T. Petrov, Accelerating reactions at the DNA can slow down transient gene expression, in: International Conference on Computational Methods in Systems Biology, Springer, 2020.
[23] D. Gillespie, Exact stochastic simulation of coupled chemical reactions, J. Phys. Chem. 81 (1977) 2340–2361.
[24] T.G. Kurtz, Limit theorems for sequences of jump Markov processes approximating ordinary differential processes, J. Appl. Probab. 8 (2) (1971) 344–356.
[25] D. Schnoerr, G. Sanguinetti, R. Grima, Approximation and inference methods for stochastic biochemical kinetics—a tutorial review, J. Phys. A, Math. Theor. 50 (9) (2017) 093001.
[26] J.R. Norris, J.R. Norris, Markov Chains, no. 2, Cambridge University Press, 1998.
[27] M.A. Shea, G.K. Ackers, The OR control system of bacteriophage lambda: a physical-chemical model for gene regulation, J. Mol. Biol. 181 (2) (1985) 211–230.
[28] M. Ptashne, A Genetic Switch: Phage Lambda Revisited, vol. 3, Cold Spring Harbor Laboratory Press, Cold Spring Harbor, NY, 2004.
[29] F. Jacob, J. Monod, Genetic regulatory mechanisms in the synthesis of proteins, J. Mol. Biol. 3 (3) (1961) 318–356.
[30] P. Boutillier, M. Maasha, X. Li, H.F. Medina-Abarca, J. Krivine, J. Feret, I. Cristescu, A.G. Forbes, W. Fontana, The kappa platform for rule-based modeling, Bioinformatics 34 (13) (2018) i583–i592.
[31] V. Danos, J. Feret, W. Fontana, R. Harmer, J. Krivine, Rule-based modelling of cellular signalling, in: CONCUR 2007–Concurrency Theory, Springer, 2007, pp. 17–41.
[32] N.E. Buchler, U. Gerland, T. Hwa, On schemes of combinatorial transcription logic, Proc. Natl. Acad. Sci. 100 (9) (2003) 5136–5141.

[33] R. Hermsen, S. Tans, P.R. ten Wolde, Transcriptional regulation by competing transcription factor modules, PLoS Comput. Biol. 2 (12) (2006) e164, https://doi.org/10.1371/journal.pcbi.0020164.
[34] J.M. Vilar, L. Saiz, DNA looping in gene regulation: from the assembly of macromolecular complexes to the control of transcriptional noise, Curr. Opin. Genet. Dev. 15 (2) (2005) 136–144.
[35] J.M. Vilar, S. Leibler, DNA looping and physical constraints on transcription regulation, J. Mol. Biol. 331 (5) (2003) 981–989, https://doi.org/10.1016/S0022-2836(03)00764-2, http://www.sciencedirect.com/science/article/pii/S0022283603007642.
[36] L. Saiz, J.M. Vilar, {DNA} looping: the consequences and its control, Curr. Opin. Struct. Biol. 16 (3) (2006) 344–350, https://doi.org/10.1016/j.sbi.2006.05.008, http://www.sciencedirect.com/science/article/pii/S0959440X06000790, Nucleic acids/Sequences and topology: Anna Marie Pyle and Jonathan Widom/Nick V Grishin and Sarah A Teichmann.
[37] L. Saiz, J.M. Rubi, J.M.G. Vilar, Inferring the in vivo looping properties of DNA, Proc. Natl. Acad. Sci. USA 102 (49) (2005) 17642–17645, https://doi.org/10.1073/pnas.0505693102, http://www.pnas.org/content/102/49/17642.full.pdf, http://www.pnas.org/content/102/49/17642.abstract.
[38] L. Saiz, J.M. Vilar, Stochastic dynamics of macromolecular-assembly networks, Mol. Syst. Biol. 2 (1) (2006).
[39] D.A. Levin, Y. Peres, E.L. Wilmer, Markov Chains and Mixing Times, American Mathematical Soc., 2009.
[40] J. Feret, T. Henzinger, H. Koeppl, T. Petrov, Lumpability abstractions of rule-based systems, Theor. Comput. Sci. 431 (2012) 137–164.
[41] M. Zukerman, Introduction to queueing theory and stochastic teletraffic models, preprint, arXiv:1307.2968.
[42] H. Bolouri, E.H. Davidson, Modeling transcriptional regulatory networks, BioEssays 24 (12) (2002) 1118–1129, https://doi.org/10.1002/bies.10189, http://www.ncbi.nlm.nih.gov/pubmed/12447977.
[43] R.W. Zeller, J.D. Griffith, J.G. Moore, C.V. Kirchhamer, R.J. Britten, E.H. Davidson, A multimerizing transcription factor of sea urchin embryos capable of looping DNA, Proc. Natl. Acad. Sci. 92 (7) (1995) 2989–2993.
[44] C.H. Yuh, H. Bolouri, E.H. Davidson, Cis-regulatory logic in the endo16 gene: switching from a specification to a differentiation mode of control, Development (Cambridge, England) 128 (5) (2001) 617–629, http://www.ncbi.nlm.nih.gov/pubmed/11171388.
[45] J.H. Levine, Y. Lin, M.B. Elowitz, Functional roles of pulsing in genetic circuits, Science 342 (6163) (2013) 1193–1200.
[46] R. Zhu, D. Salahub, Delay stochastic simulation of single-gene expression reveals a detailed relationship between protein noise and mean abundance, FEBS Lett. 582 (19) (2008) 2905–2910, https://doi.org/10.1016/j.febslet.2008.07.028, http://www.sciencedirect.com/science/article/pii/S0014579308006194.
[47] Y. Lin, C.H. Sohn, C.K. Dalal, L. Cai, M.B. Elowitz, Combinatorial gene regulation by modulation of relative pulse timing, Nature 527 (7576) (2015) 54–58, https://doi.org/10.1038/nature15710, http://www.ncbi.nlm.nih.gov/pubmed/26466562.
[48] O. Radulescu, S.S. Samal, A. Naldi, D. Grigoriev, A. Weber, Symbolic dynamics of biochemical pathways as finite states machines, in: International Conference on Computational Methods in Systems Biology, Springer, 2015, pp. 104–120.
[49] R. Vivek-Ananth, A. Samal, Advances in the integration of transcriptional regulatory information into genome-scale metabolic models, Biosystems 147 (2016) 1–10.
[50] G.d.C.P. Innocentini, M. Forger, A.F. Ramos, O. Radulescu, J.E.M. Hornos, Multimodality and flexibility of stochastic gene expression, Bull. Math. Biol. 75 (12) (2013) 2360–2600.
[51] K. Parmar, K.B. Blyuss, Y.N. Kyrychko, S.J. Hogan, Time-delayed models of gene regulatory networks, Comput. Math. Methods Med. (2015).
[52] K. Greenham, C.R. McClung, Time to build on good design: resolving the temporal dynamics of gene regulatory networks, Proc. Natl. Acad. Sci. 115 (25) (2018) 6325–6327.
[53] A.N. Goban, O. Radulescu, Dynamic and static limitation in multiscale reaction networks, revisited, Adv. Chem. Eng. 34 (2008) 103–107.
[54] M. Pájaro, I. Otero-Muras, C. Vázquez, A.A. Alonso, Transient hysteresis and inherent stochasticity in gene regulatory networks, Nat. Commun. 10 (1) (2019) 1–7.
[55] J. Casadesús, R. D'Ari, Memory in bacteria and phage, BioEssays 24 (6) (2002) 512–518.
[56] B. Nashun, P.W. Hill, P. Hajkova, Reprogramming of cell fate: epigenetic memory and the erasure of memories past, EMBO J. 34 (10) (2015) 1296–1308.

Further reading

[57] R. Milo, P. Jorgensen, U. Moran, G. Weber, M. Springer, Bionumbers—the database of key numbers in molecular and cell biology, Nucleic Acids Res. 38 (suppl 1) (2010) D750–D753.
[58] J.M. Vilar, L. Saiz, Suppression and enhancement of transcriptional noise by DNA looping, Phys. Rev. E 89 (6) (2014) 062703.
[59] Y. Harada, T. Funatsu, K. Murakami, Y. Nonoyama, A. Ishihama, T. Yanagida, Single-molecule imaging of rna polymerase-dna interactions in real time, Biophys. J. 76 (2) (1999) 709–715.
[60] M. Brunner, H. Bujard, Promoter recognition and promoter strength in the Escherichia coli system, EMBO J. 6 (10) (1987) 3139.
[61] B. Müller-hill, Lac Operon, Wiley Online Library, 1996.
[62] J.M. Vilar, S. Leibler, DNA looping and physical constraints on transcription regulation, J. Mol. Biol. 331 (5) (2003) 981–989.